

Factors controlling mechanical properties of clay mineral/polypropylene nanocomposites

A. OYA*, Y. KUROKAWA

Faculty of Engineering, Gunma University, Kiryu, Gunma 376-8515, Japan

E-mail: oya@chem.gunma-u.ac.jp

H. YASUDA

Calp Corporation, Sodegaura, Chiba 299-0205, Japan

Effects of two factors on the mechanical properties of clay mineral/polypropylene nanocomposites were examined. The first factor is the presence of a small amount of poly(diacetone acrylamide) formed between clay mineral layers. This material was expected to separate effectively the stacked layer structure of the clay mineral on mixing with polypropylene. The stacked layer structure, however, was not separated sufficiently in spite of expansion of the interlayer distance of clay mineral, leading to poor improvement of the mechanical properties of the nanocomposite. Another factor is the kind of clay mineral. Montmorillonite and mica resulted in less favorable separation of the stacked structure than hectorite, but the resulting nanocomposites gave outstanding improvement of the properties. The stiffness of clay mineral layer was considered to influence the properties of the nanocomposite strongly. © 2000 Kluwer Academic Publishers

1. Introduction

Toyota group has developed montmorillonite (a clay mineral)/nylon nanocomposite with excellent mechanical properties [1, 2], which aroused our interest to use clay mineral as a reinforcement material for polymers. The nanocomposite contained separated montmorillonite layers throughout the nylon matrix homogeneously. However this nanocomposite has been scarcely used practically contrary to our expectation because of a too tedious preparation procedure leading to a high cost. Later Giannelis *et al.* developed a simple preparation procedure of nanocomposite in which clay mineral intercalated with organic cations was fused together with a polymer [3, 4], but the procedure was applicable to only polar polymers successfully and not nonpolar ones such as polypropylene which is one of the most important matrix materials from a practical point of view.

In order to complete the requirement the present authors developed a novel but somewhat complex procedure consisting of three steps as follows [5, 6]; i) a small amount of polymerizing polar monomer, diacetone acrylamide, was intercalated between clay mineral layers and then polymerized to expand the interlayer distance, ii) polar maleic acid-modified polypropylene, in addition, was intercalated into the interlayer space to make a composite used as “master batch”, iii) the master batch was finally mixed with a conventional polypropylene to prepare a nanocomposite. Maleic acid-modified polypropylene was expected to expand the interlayer distance further and also to improve the affinity be-

tween clay mineral and polypropylene, possibly leading to improvement of mechanical properties.

Two nanocomposites have been prepared according to the above procedure by using hectorite and montmorillonite as a filler mineral, but their mechanical properties, especially of the former one, were not improved to our expectation [5, 6]. We thought two causes were responsible for these poor results: one is the presence of a small amount of polymerized diacetone acrylamide between the clay mineral layers, and another is that the clay minerals used were too flexible to give desired reinforcement effects. Later we found a nanocomposite can be prepared without diacetone acrylamide and consequently it became possible to examine the first cause. Thus the present work was carried out to make clear above two causes, for which some data reported previously were taken up again for the comparison [5, 6].

2. Experimental procedures

2.1. Materials

The following three clay minerals were used in the present work.

1) Hydrophobic hectorite (Corp Chemical Ind. Co., abbreviation: HC): Synthesized hectorite was ion-exchanged with quaternary ammonium cations. The ideal chemical formula is $X_{0.33}^+(Mg_{2.67}Li_{0.33})Si_4O_{10}(OH)_2$, here X^+ is $(CH_3)_3N^+R$ and $(CH_3)_2N^+RR'$; and $R=C_{16}H_{33}$, $R'=C_{18}H_{37}$.

* Author to whom all correspondence should be addressed.

2) Hydrophobic montmorillonite (Kunimine Ind. Co., abbreviation: MM): Natural montmorillonite was ion-exchanged with the quaternary ammonium cations. The ideal chemical formula is $X_{0.33}^+(Al_{1.67}Mg_{0.33})Si_4O_{10}(OH)_2$, here X^+ and R in X^+ are the same as in HC, respectively.

3) Hydrophobic mica (Corp Chemical Ind. Co., abbreviation: MC): K^+ in synthesized mica with an ideal chemical formula $K_xMg_{3-\frac{x}{2}}Si_4O_{10}F_2$ ($x=0.5-0.8$) was ion-exchanged with the quaternary ammonium cations of R and R' being the same as in HC. Diacetone acrylamide ($CH_2=CHCONHC(CH_3)_2CH_2COCH_3$; abbreviation: DAAM) and 2,2'-azobis(isobutyronitrile) ($(CH_3)_2C(CN)N=NC(CN)(CH_3)_2$, abbreviation: AIBN) were used as a polymerizing polar monomer and a polymerization catalyst for it, respectively. In addition, a conventional polypropylene (a 1 : 1 mixture of J700GP and H700 supplied by Calp Corporation, abbreviation: PP) and maleic acid-modified PP with 10 wt% of maleic acid (YUMEX 1010 supplied by Sanyo Chemical Industries, abbreviation: m-PP) were used.

2.2. Preparation procedures of nanocomposites

In addition to the conventional PP without filler and talc/PP composite used as a reference, four nanocomposites were prepared in the previous and the present works according to methods A or B shown in Fig. 1. The composites are shown with the appendices of (A) or (B).

1) HC/PP(A): Method A has been explained elsewhere in detail [5] so that the preparation procedure of HC/PP will be described briefly. A toluene solution of DAAM was mixed with a toluene solution of HC in which AIBN was intercalated in advance, kept for 1hr at 30°C for intercalation of DAAM and subsequently

kept at 75°C for 1 hr to polymerize DAAM, during the treatments the solutions were stirred under N_2 atmosphere. The toluene solution after the polymerization treatment was mixed with a m-PP toluene solution and heated to 100°C with stirring for intercalation of m-PP. The resulting solution after cooling down to 60 °C was dropped into methanol, and the deposited pasty material was washed repeatedly with methanol and finally dried to obtain a master batch. The master batch and the conventional PP was mixed together by a twin screw extruder (Ikegami, PCM30) and finally shaped into some specimens for measurement with a Nissei Jyushi Kogyo FE120S.

2) HC/PP(B): This composite was prepared according to method B. Toluene solutions of HAN and m-PP were mixed at 100°C for 1hr under N_2 atmosphere and then subjected to the same procedures as used for the HC/PP(A) composite.

3) MM/PP(A): The composite was prepared according to the same processes for HC/PP(A) excepting for the use of MM instead of HC, of which details were reported elsewhere [6].

4) MC/PP(B): MC was used as a filler. The procedures are the same as those used for HC/PP(B).

2.3. Measurements

1) X-ray diffraction was carried out with Rigaku Geigerflex by using Ni-filtered $Cu K\alpha$. X-ray parameters of interlayer distance (d_{001}) and crystallite thickness (L_c) of the clay mineral were calculated from the (001) diffraction peak.

2) A transmission electron microscope, Phillips CM30, was used to observe the physical state of clay minerals before and after using as a filler material. An ultrathin section of 50 nm in thickness was prepared by a ultramicrotome EM-Supernova.

3) The properties of the resulting nanocomposites were measured as follows; Bulk density was measured

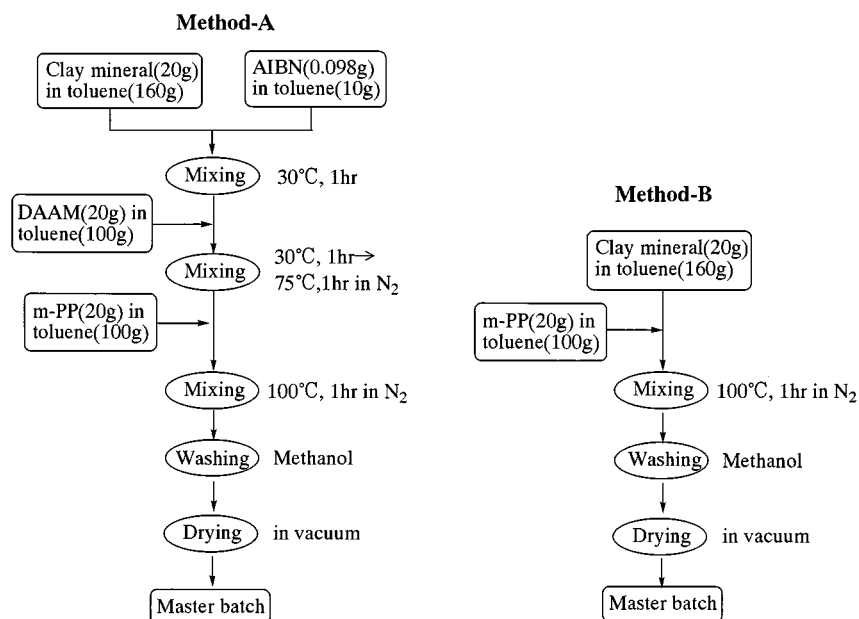


Figure 1 The nanocomposite specimens prepared for measurement of some properties.

TABLE I Interlayer distances (d_{001}) and crystallite thickness (L_c) of pristine clay minerals and those in the nanocomposites

	d_{001} (nm)	L_c (nm)
HC	2.49	10.0
HC/PP(A)	3.98	11.4
MM	3.80	35.3
MM/PP(A)	3.80	18.5
HC	2.49	10.0
HC/PP(B)	2.26	9.1
MC	3.43	19.6
HC/PP(B)	2.69	18.6

by Archimedes's method. Tensile strength was measured according to ASTM D-638 with a Toyo Seiki Stograph. Bending strength and bending modulus were measured under ASTM D-790. The apparatus used is a Toyo Seiki Bendgraph. For notched IZOD impact strength, a Toyo Seiki IZOD impact strength machine was used under ASTM D-265. Heat distortion temperature (HDT) was measured with a Toyo Seiki Full Automatic HTD tester under ASTM D-648.

3. Results and discussion

3.1. Structures of pristine clay minerals

The X-ray diffraction profiles of the clay minerals are shown in Fig. 2, and X-ray parameters calculated from the (001) peaks are summarized in Table I. HC gave the broadest (001) peak among three clay minerals and its (002) peak was so equivocal. Before starting the present work, we expected that the sharpest peak would be given by MC, but MM showed the sharpest peak as shown in Fig. 2.

There were large differences among the interlayer distances (d_{001}) of three clay minerals in spite of the intercalation with same quaternary ammonium cations. A clay mineral with a larger d_{001} , in general, has a larger crystallite thickness (L_c). The average number of layers constituting a clay mineral crystallite, L_c/d_{001} , are 4.0, 9.3, 5.7 for HC, MM and MC, respectively.

Fig. 3 shows the TEM photographs of the pristine clay minerals. The well-developed crystalline layer structures were observed in both MM and MC, whereas the HC showed a loosely stacked layer structure. Comparison among three photographs suggests that the HC layers are somewhat shorter and more flexible, in other words less stiff, than other two layers.

3.2. Structures of nanocomposites

Fig. 4 shows X-ray diffraction profiles of the nanocomposites prepared in the present work, in addition to those reported previously [5, 6]. It is reasonable to say that the diffraction peaks of clay minerals in the composites are broader than those of their corresponding pristine ones, which means that the stacked layer structures of pristine clay mineral were separated in thinner ones through the preparation processes of the nanocomposites. This figure also indicates that the (001) X-ray diffraction profile was broader in the order of MM/PP(A), MC/PP(B), HC/PP(A) and HC/PP(B); the last one has no peak.

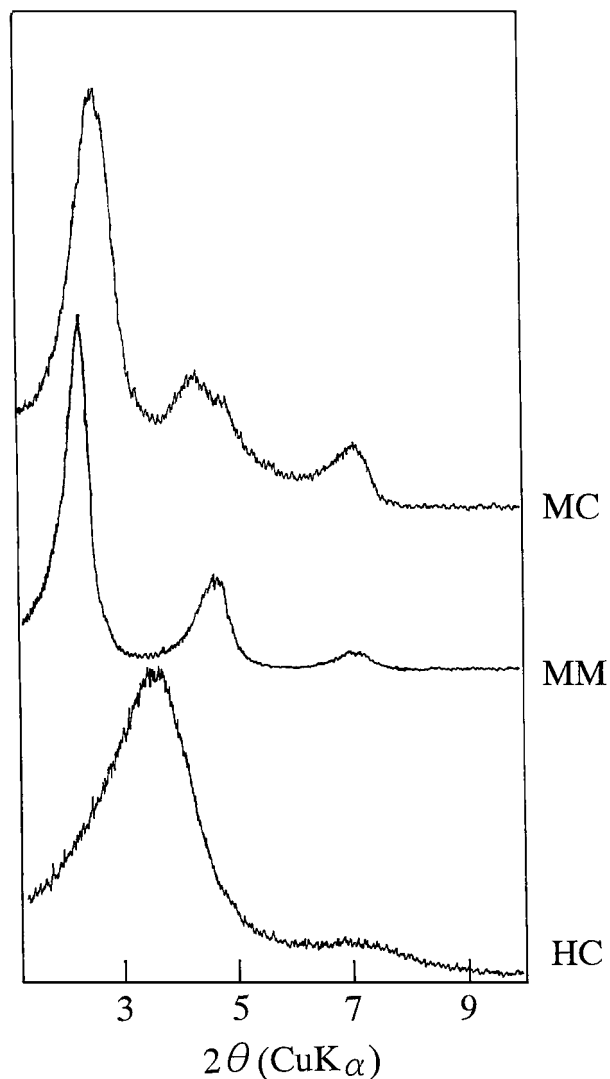


Figure 2 X-ray diffraction profiles of the pristine clay minerals.

This order shows that a lower crystalline clay mineral structure is separated more easily.

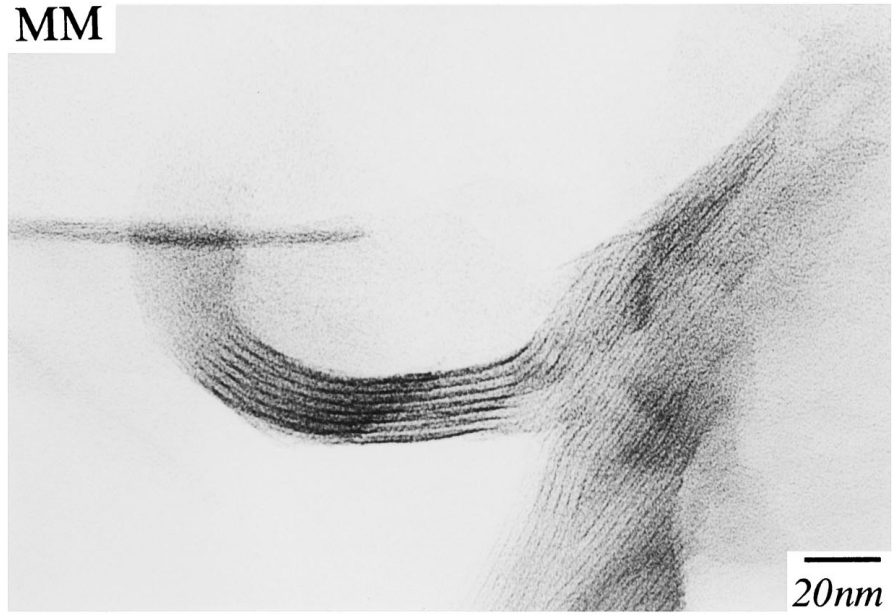
Table I shows X-ray parameters of the clay minerals in the composites. Since the content of clay mineral was controlled to be 3 wt%, the diffraction peaks were quite weak, leading to somewhat unreliable X-ray parameters. Nevertheless one tendency can be deduced from Table I, that is, the clay minerals in the composites by method A have larger (or nearly equal) d_{001} values than those of the pristine ones. Opposite results were observed in the case of method B. The formation of polymerized DAAM between the layers suppressed the shrinkage of interlayer distance during the preparation process of nanocomposite.

Fig. 5 shows the TEM photographs of the nanocomposites. As suggested from X-ray diffraction profiles well-separated layers are observed in both HC/PP(A) and HC/PP(B). Many of them are stacked two or three layers deep, and the monolayers are also observed. The layers have nearly equal length to that of the pristine one so that HC layers were not cut, though were separated, through the preparation processes. HC layers in the composite were relatively shorter and seem to be less stiff than those of MM and MC as well as in the cases of the pristine clay minerals.

HC



MM



MC



Figure 3 TEM photographs of the pristine clay minerals.

The TEM photographs showed that the thickly stacked layer structures were separated into thinner ones in MM/PP(A) and MC/PP(B) through the preparation processes of the nanocomposite, though not so perfectly as in HC/PP(A) and HC/PP(B). These separated layer structures are strictly flat, without bending or wrinkling, and seem to be stiffer than the HC layer.

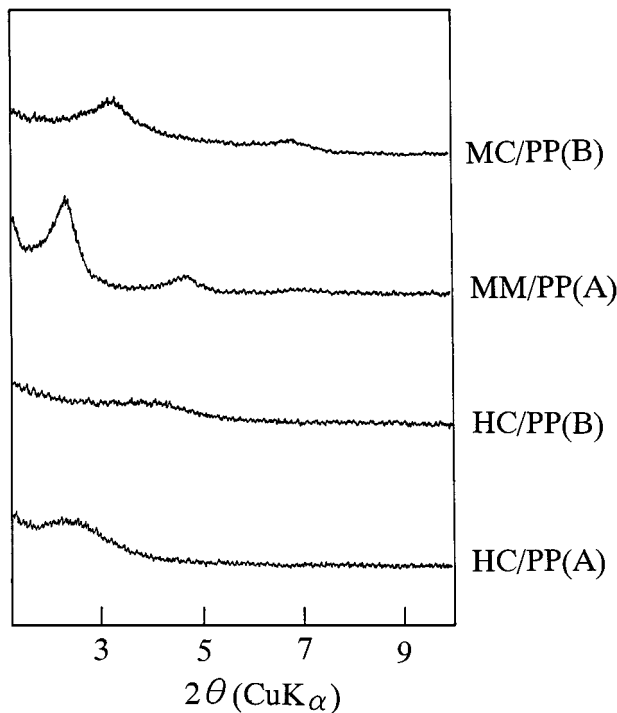
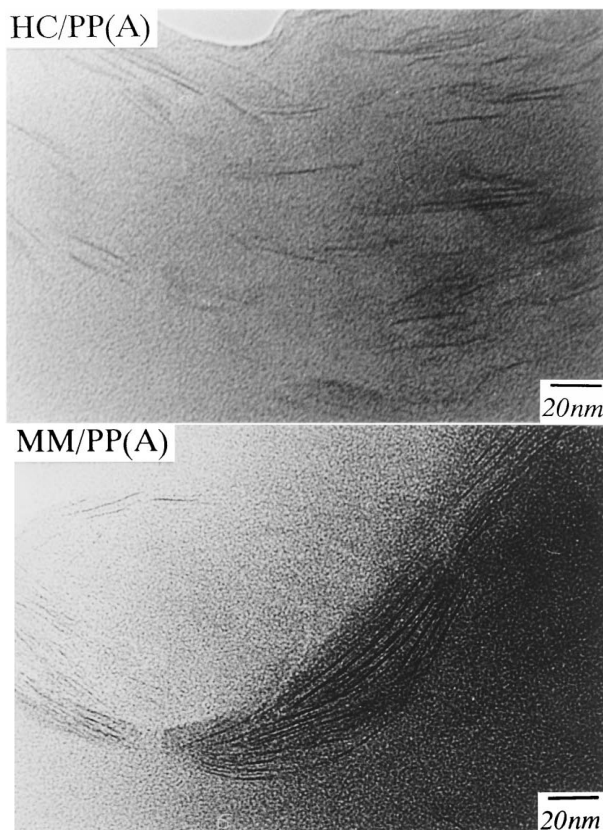


Figure 4 X-ray diffraction profiles of the nanocomposites.



3.3. Properties of nanocomposites

The properties of the nanocomposite, together with those of the conventional PP and a talc/PP composite, are summarized in Table II. The filler content was controlled to be 3 wt% in all composites. It should be emphasized that clay minerals exhibited more desirable reinforcement effects than talc which is a conventional reinforcement material. Maiti and Sharma [7] reported that the tensile strength and tensile modulus of a conventional talc/PP composite decreased and increased with increasing of the talc content respectively, although values were not reported concretely. The data in Table II are discussed from two points below.

4. Discussion and conclusions

4.1. Effects of polymerized DAAM

As confirmed in Table I, the presence of polymerized DAAM acted to keep a large interlayer distance (d_{001}) of clay mineral after the preparation of the nanocomposite. This behavior, we expected initially, leads to preferable separation of the stacked layers in the resulting nanocomposite. Based on the data shown in Fig. 3, however, method B showed a more diffused X-ray diffraction profile. Thus we can conclude that the presence of polymerized DAAM may or may not lead to more preferable separation of clay mineral stacked layers. Another point to be discussed is to make clear the effects of polymerized DAAM on the properties of nanocomposite, which will be revealed through the comparison between HC/PP(A) and HC/PP(B). Both the composites gave almost equal values in all properties excepting for notched IZOD impact strength. It

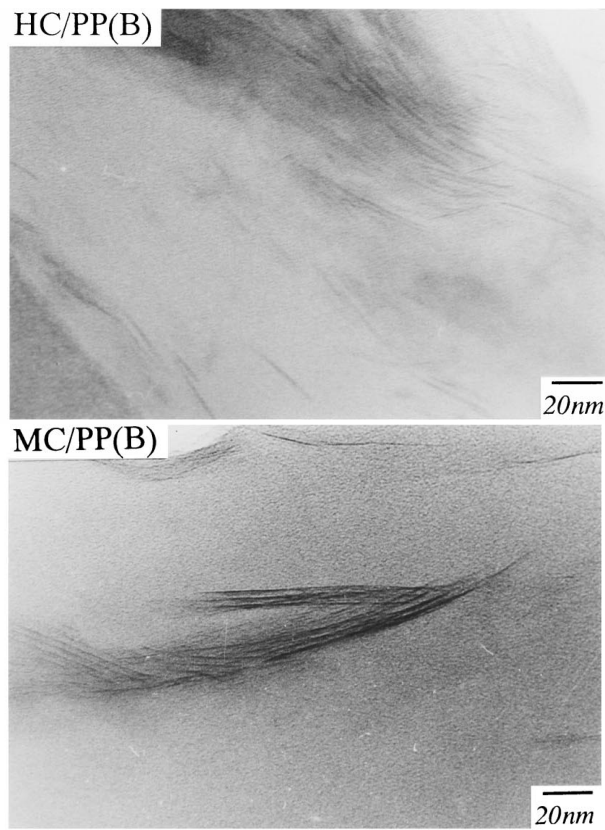


Figure 5 TEM photographs of the nanocomposites.

TABLE II Properties of PP with and without fillers

	PP	Talc/PP	HC/PP(A)	MM/PP(A)	HC/PP(B)	MC/PP(B)
Content of inorganic matter (wt%)	0	3	3	3	3	3
DAAM	—	no	yes	yes	no	no
Density (kg m ⁻³)	910	920	930	930	930	930
Tensile strength (MPa)	31	35	37	39	35	39
Bending strength (MPa)	38	45	48	53	49	55
Bending modulus (MPa)	1500	1900	2000	2100	2020	2500
IZOD impact strength (with notch) (kJm ⁻²)	2.0	2.1	2.3	3.4	2.9	3.9
HDT (°C) ^a	120	—	125	130	125	132

^aHeat distortion temperature.

will be concluded that the presence of polymerized DAAM has no effects substantially on the properties of the nanocomposite. This technique could be used for preparation of clay mineral/polymer nanocomposites.

4.2. Effects of kind of clay mineral

Higher reinforcement effects were achieved in both MM/PP(A) and MC/PP(B) than in the HC-reinforced composites in spite of the poorer separation of the stacked structures. These results are completely opposite to our initial expectation. There must be other factors influencing the properties of the nanocomposite more strongly. The effects of size and stiffness of a clay mineral layer were suggested.

It is well known that a clay mineral filler with a larger aspect ratio exhibits more preferable reinforcement effects on the resulting composite [8], but we could not measure the crystallite size (L_a) from X-ray diffraction profiles of the composites. Another way is to use the TEM photographs. Both the MM and MC have larger layer lengths but simultaneously have thicker layer stacking. So it was also difficult to evaluate the aspect ratios of clay minerals in the composites. Another possibility is the stiffness of clay mineral layers. No data on the stiffness of the clay mineral layer are available at present. It is reasonable to deduce from the results stated above, however, that the MM and MC layers seem to be more stiff than the HC layer as stated above. The properties of the nanocomposite are con-

trolled more strongly by the stiffness of the clay mineral layer. This idea will be supported by a large bending modulus of MC/PP(B), because this property, in general, is improved remarkably by using a stiff reinforcement material. When the data in Table II are considered on the basis of the above discussion MC must be stiffer than MM.

As a result, a nanocomposite with excellent mechanical properties is prepared through preferable separation of stiff clay mineral layers throughout a matrix.

References

1. Y. FUKUSHIMA, A. OKADA, M. KAWASUMI, T. KURAUCHI and O. KAMIGAITO, *Clay Miner* **23** (1988) 27.
2. A. USUKI, Y. KOJIMA, M. KAWASUMI, A. OKADA, Y. FUKUSHIMA, T. KURAUCHI and O. KAMIGAITO, *J. Mater. Res.* **8** (1993) 1179.
3. R. A. VAIA, H. ISHII and E. P. GIANNELIS, *Chem. Mater.* **1993** (5) 1694.
4. E. P. GIANNELIS, *Adv. Mater.* **8** (1996) 29.
5. Y. KUROKAWA, H. YASUDA and A. OYA, *J. Mater. Sci. Lett.* **15** (1996) 1481.
6. Y. KUROKAWA, H. YASUDA, M. KASHIWAGI and A. OYA, *ibid.* **16** (1997) 1670.
7. S. N. MAITI and K. K. SHARMA, *J. Mater. Sci.* **27** (1992) 4605.
8. J. LUSIS, R. T. WOODHAMS and M. XANTHOS, *Polym. Eng. & Sci.* **13** (1973) 139.

Received 11 August
and accepted 25 August 1999